Composites: Part A 200 (2026) 109339

Contents lists available at ScienceDirect

Composites Part A

journal homepage: www.elsevier.com/locate/compositesa

Flame-retardant composites and analysis of their residual strengths after tailored flame tests☆

Melissa Walter *, Antonia Jarchow, Bodo Fiedler

Hamburg University of Technology, Institute of Polymers and Composites, Denickestraße 15, 21073 Hamburg, Germany

GRAPHICAL ABSTRACT

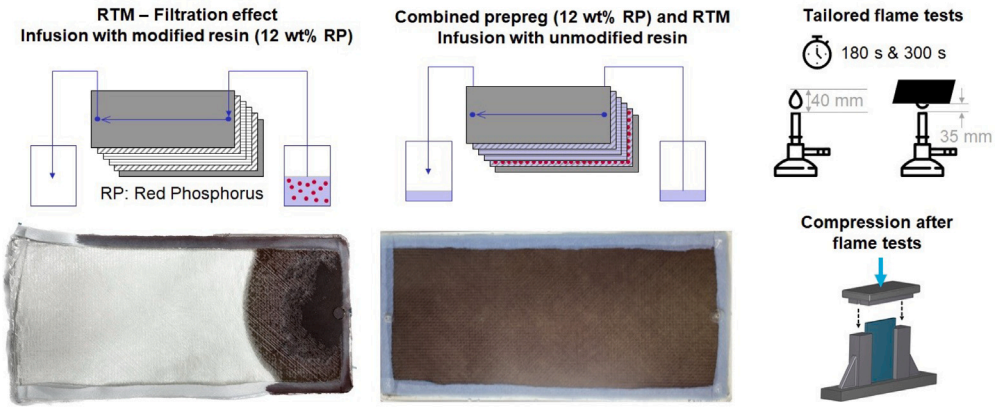

ARTICLE INFO

Keywords:
Flame behaviour
Red phosphorus
Lightweight design
Sustainability
Co-curing
Material savings

ABSTRACT

In recent decades, fibre-reinforced polymers (FRPs) have become a key factor to realise lightweight design, e.g., to safe fuel in mobility applications. As FRPs are usually combustible, flame retardants (FRs) are necessary to fulfil critical requirements. On the one hand, FRs can negatively affect thermo-mechanical properties of composites and should therefore used as little as possible. On the other hand, frequently used infusion processes to manufacture FRPs are no longer possible due to filtration effects, if the FRs are present as particles. However, novel in this study is the use of a combined prepreg and infusion process to solve both challenges by implementing FRs only in the most exposed plies. Simultaneously, this method enables the manufacturing of large parts with implemented FR particles, without compromising the lightweight potential or causing adhesion challenges through the use of FR gel-coats. As part of this study, tailored flame tests with adequate reproducibility were developed for qualitative comparisons between different configurations and the residual compressive strength was determined afterwards, because the structural integrity in fire scenarios is of special importance in mobility applications. It was found, that despite a very low global amount of ≈ 1.5 - 3 % red phosphorus leads to significant improvements in the residual strength compared to unmodified configurations.

☆ This article is part of a Special issue entitled: 'CompTest 2025' published in Composites Part A.

* Corresponding author.
E-mail address: melissa.walter@tuhh.de (M. Walter).

https://doi.org/10.1016/j.compositesa.2025.109339
Received 28 July 2025; Received in revised form 11 September 2025; Accepted 3 October 2025
Available online 13 October 2025

1. Introduction

In the case of fires, the protection of people is a priority. The structural integrity of e.g. train walls has to be maintained long enough to enable people to evacuate the affected zone. FRPs are increasingly being used to conserve resources and fuel because their high specific strength and stiffness make them ideal for lightweight design. e.g. in mobility applications. However, unlike metal materials, most FRPs are not inherently flame-retardant, necessitating the addition of flame retardants (FRs), which are often added as particles.

Resin transfer moulding (RTM) is a widely used manufacturing process for large composite parts with the advantage of relatively low tooling costs and high surface qualities [1,2]. The addition of particle fillers to the matrix is used to enhance or provide supplementary properties, e.g. flame retardancy [3,4]. The distribution of the particles in the laminate is usually decisive for these properties.

In infusion processes, particles with the size of tens of microns lead to filtration effects [5–8] with an inhomogeneous particle distribution or in worst case to inadequate final component [9,10]. In general, larger particle sizes or agglomeration as well as rising fibre-volume contents increase filtration effects [10].

Filtration effects can be divided in different types, where cake filtration and deep bed filtration are the most common phenomena [7, 11,12]. When particle sizes are larger than the available pore size, macroscopic cake filtration occurs where deposited particles build-up ahead of the fibres as soon as the dispersion enters the mould. Along the reinforcement length, microscopic cake filtration may appear due to different scales of inter and intra tow channels [9]. If particles dimensionally smaller than the pore channels are captured, deep bed filtration occurs, which not only results in particle gradients but also in extended infusion times [9].

In addition to the challenges with filtration effects, particles in the micrometre range often influence the thermo-mechanical properties. While the toughness can be improved due to their implementation, most other properties e.g. the glass-transition temperature or strength often decrease [13–16], as particles in this size can act as defects [17, 18], 'disturb' the network structure of polymers and also worsen the fibre-matrix bonding in FRPs [19]. Minimal use is therefore desirable to minimise the impact on thermo-mechanical properties.

In order to minimise the proportion of flame retardants required in composites, current studies often focus on combining different flame retardants [20–23] to exploit synergistic effects, but also on microencapsulations [24,25] to make flame retardants more efficient. Especially when using carbon and natural fibres, surface modifications for fibres [26,27] or interlayer nanofibre methods [28] are under investigation.

In the case of FR-particles, implementation in fire-exposed sections, e.g. on component surfaces, is most effective. The use of gel coats or coatings is one way to achieve surface flame retardancy in industrial practice [29]. However, the use of additional material can limit the potential for lightweight design [30] and is sometimes not possible due to restricted mounting circumstances [31]. Additionally, gelcoat-based methods can undergo swelling, and shape or mechanical distortion and their application lead to an additional interphase, which may lead to challenges regarding adhesion [32].

Based on conventional composite manufacturing methods like infusion and prepreg/autoclave processes, methods have been developed to combine the advantages of both processes. Prepregs (pre-impregnated fibres) are generally used to achieve high mechanical performance, while infusion methods are e.g. cost-efficient. The *Combined Prepreg and Infusion Technology* (CPI) is generally used for highly stressed components that are large and have complex geometries. Prepregs are used for geometrically simple areas exposed to high mechanical loads, while complex structures such as stringers or frames are manufactured using infusion processes (e.g. RTM). Both parts are combined in the same curing cycle, which increases integration and cost efficiency. However, the interface quality between prepreg and infusion part is relevant for the mechanical performance of the component [33–35].

To evaluate the residual strength after different damage types, the mechanical properties of damaged specimens are compared to the initial, undamaged state. For FRPs, most studies investigate the influence of low-velocity impacts, e.g., with the standardised compression after impact test (CAI, ASTM D7137) [36,37]. The determination of residual strength after flame tests is reported primarily for metals and (steel) concrete, especially due to their use in the construction sector [38,39]. Some studies also address the residual strength of composites after flame treatment. Yang et al. [40] and Vieille et al. [41] investigated the tensile strength properties remaining after a fire and concluded that the flame-retardant additive not only delays the thermal degradation of carbon fibre-reinforced PEKK laminates, but also contributed efficiently to maintaining the structural integrity of the composites, and that the residual tensile strength after quasi-isothermal pyrolysis in an inert environment decreases linearly with increasing pyrolysis degree for carbon fibre-reinforced phthalonitrile composites. Sorathia et al. [42] analysed the residual flexural strength during and after fire exposure. Residual compressive strengths were evaluated after lightning strike scenarios by Millen et al. [43] and Wang et al. [44]. It was found, that mechanical damage to the individual plies, due to the combined effects of mechanical and thermal strains during the strike had a significant effect on the residual strength.

This study is based on the promising results on heterogeneous flame-retardant wet layups published in [45]. In this work, it was shown that a minimal global flame retardant content is sufficient to improve the flame retardant properties of GFRPs as long as they are present on the surface of the composite.

The aim of this study is to examine the feasibility of a CPI method to enable the transfer to automated and industrially suitable manufacturing for FRPs with FR particle-loaded resins. When FRs are located directly within the composite, gelcoats or coatings can fulfil additional functionalities in combination with a CPI-process (e.g., resistance to hydrolysis or UV radiation), extending the service life of the respective component. Flame tests with a minimum of measuring equipment will be presented for qualitative comparison. The residual strength of the flame-treated composites is tested to investigate the structural integrity which is relevant in many applications in the event of a fire.

2. Materials and methods

2.1. Materials

The DGEBA Resin *827* (*EPIKOTE® 827*, Westlake, Houston, USA) is mixed stochiometrically with the amine curing agent *137H* (*EPIKURE® RIMH 137*, Westlake, Houston, USA). *RP* (Red Phosphorus, *Exolit RP 607*, Clariant, Muttenz, Suisse) is added as a flame retardant. Composites were manufactured using biaxial E-glass-fibre fabrics (610 gsm, SAERTEX GmbH & Co. KG, Saerbeck, Germay). A 30 g/m^2 non-woven (*NW*, R&G Faserverbundwerkstoffe GmbH, Waldenbuch, Germany) was partly added on the surfaces.

2.2. Manufacturing

Fig. 1 displays the manufactured and investigated quasiisotropic $[\pm45°, 90°, 0°, \pm45°, 90°, 0°]_s$ laminates, partially containing NWs on the surface. The investigated configurations and share of RP in the matrix were determined based on UL94 tests of RP-modified epoxy without fibre-reinforcement as well as on the results of preliminary studies using wet-layups published in [45].

Resin transfer moulding (RTM) with 1 bar of vacuum during and 2 bar pressure after infusion is used for unmodified configurations. A closed aluminium mould with dimensions of 600 mm x 300 mm x 4 mm is used. The process includes curing for 8 h at 50 °C in a heat press

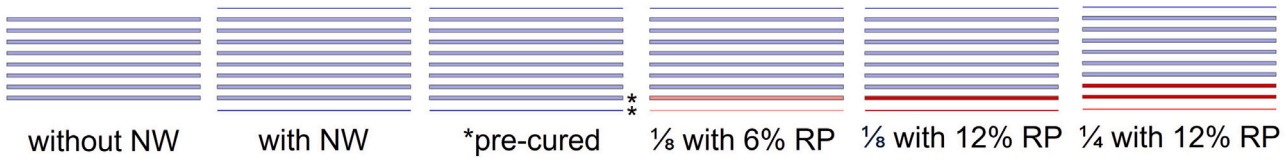

Fig. 1. Schematic illustrations of investigated heterogeneously modified laminates. (Thick line: Biaxial glass-fibre fabric; thin line: NW; blue: unmodified; light red: 6 wt. % RP; dark red: 12 wt. % RP. All modified plies are pre-impregnated and pre-cured. Unmodified plies are infused in their dry state, except plies marked with *.).

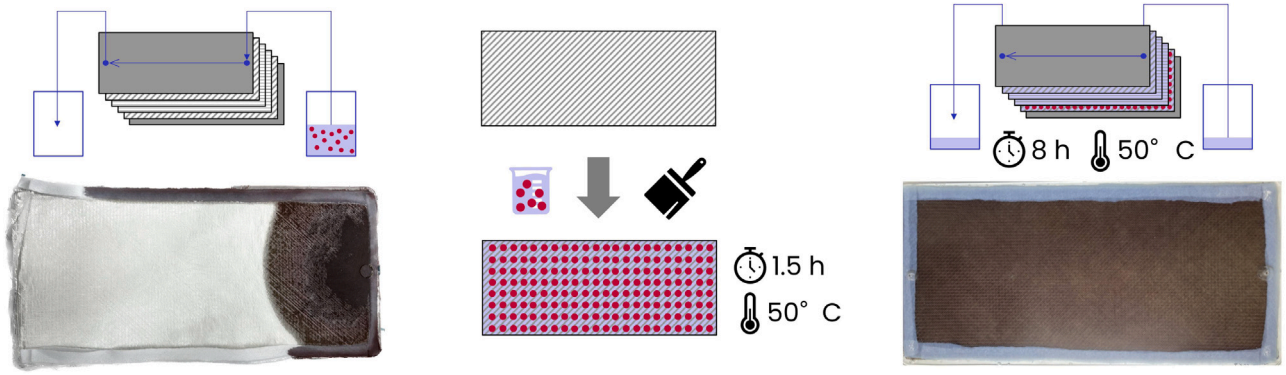

Fig. 2. Incompletely infused plate due to the filtration effect during the RTM process with RP-loaded resin (left), wet lay-up of the modified layers (centre) and combined prepreg and infusion process to avoid filtration effects (right).

and post-curing for 16 h at 80 °C in a convection oven *UF 450plus* (Memmert GmbH & Co. KG, Büchenbach, Germany).

Due to an occurring filtration effect mentioned in Section 1, it is not possible to manufacture panels with RP-loaded epoxy resin (see Fig. 2). This is why this study uses a CPI-method to manufacture GFRPs containing heterogeneous distributed RP. Before the RTM process with unmodified epoxy resin, modified plies are impregnated by hand and pre-cured as illustrated in Fig. 2.

Based on thermokinetic methods, the author investigated the curing behaviour of the used resin system in [46]. The procedure and an experimental validation using FT-IR and DSC measurements are described in detail in [46]. From these investigations and the results of preliminary studies published in [45], a pre-curing time of the modified layers of 90 min at 50 °C could be determined, which corresponds to a pre-curing of ≈ 45 %. In order to investigate any potential influence of pre-curing independent of additional particle loading, an unmodified plate was also pre-impregnated and pre-cured with pure resin.

2.3. Reproducibility, traceability and specimen preparation

Two plates are manufactured for each configuration to ensure reproducibility. For tracability and comparability, test specimens are uniformly extracted and labelled. A *F45* circular saw (Altendorf GmbH & Co. KG Maschinenbau, Minden, Germany) with diamond saw blade is used for edging the plates. A CNC-saw *Brillant 265* (ATM Qness GmbH, Mammelzen, Germany) with a diamond saw blade and water cooling is utilised to cut the test specimens according to the resp. standards.

2.4. Tailored flame tests

In order to assess the fire behaviour of composite materials, a variety of standardised tests can be carried out. As realistic room fire tests are very expensive, the fire behaviour of smaller specimens can be tested under controlled conditions on lab-scale. The influencing parameters of specimen geometry, ignition source, oxygen supply and heat yield can be specified, allowing different materials to be compared, classified and certified. Frequently used and simple tests can be performed according to UL 94 (Underwriters Laboratories, Northbrook, Illinois, USA), where samples are flamed twice for 10 s with a defined bunsen burner flame, e.g., in a vertical flame test. After each flame treatment, the after-flame time is noted and the dripping of the material is analysed, allowing different classifications of the material as a result.

However, as FRPs are usually only exposed to potential flames on the surface and not over their cross-section, horizontal tests are more realistic for mobility applications. For standardised horizontal tests, such as cone calorimetry, special equipment is necessary, e.g., to capture the heat release rates. However, the tailored flame tests, that are performed in this study, focus on qualitative comparisons between the manufactured configurations with minimal equipment and have been developed based on various flame tests, as described in [45]. In short, the time-to-ignition (tti) and the mass loss of the sample are determined as usual in cone calorimetry. The sample is clamped horizontally over a Bunsen burner and a metal mould is used as a holder, which itself is non-combustible and corrosion-resistant, as described in the "Aircraft Materials Fire Test Handbook". Other standards, such as ASTM F776 according to DOT/FAA/AR-00/12 and DIN EN 60695-11-10, also provide methods for analysing horizontally tested test specimens, whereby different fire lengths are examined.

Specifically, the 40 mm flame of a bunsen burner (0,7 kW, methane gas, technical grade) is applied centred at a distance of 35 mm to the surface of 100 mm x 150 mm specimens with 4 mm thickness for 180 s resp. 300 s. Four specimen are flamed for each configuration and length of flame treatment. A horizontally aligned steel frame is used to avoid edge effects due to a spreading flame. Temperature measurements are conducted every 5 s at three positions (1. flamed surface aside from the flame at the edge, 2. middle of opposite side and 3. steel frame) using Type K thermoelements (TC Mess- und Regeltechnik GmbH, Mönchengladbach, Germany). The flame tests are performed in a *HVFAA Horizontal Vertical Flame Chamber* (Atlas Material Testing Technology, Mount Prospect, Illinois, USA). Videos are recorded during the tests. Herewith, the time-to-ignition and after-flame time is analysed for every specimen. Furthermore, mass loss is tracked. The set-up is visible in the supplementary information.

2.5. Mechanical characterisation

2.5.1. Three-point bending tests

Three-point bending (3PB) tests are performed based on DIN EN ISO 14125 on a universal testing machine *Allroundline Z10* (Zwick Roell, Ulm, Germany) with 3 mm/min. The investigated 3PB-specimens have a geometry of 120 mm x 15 mm and a test length of 80 mm, while the supports have a diameter of 10 mm. For each configuration, ten specimens are tested with the pre-cured part on the tensile side as well as on the compression side.

2.5.2. Compression tests

Compression tests are conducted according to DIN EN ISO 14126 on a *Allroundline Z400* (Zwick Roell, Ulm, Germany). The specimens have geometries of 140 mm x 10 mm x 4 mm. According to the 4th Euler buckling case, the free test length is calculated to 10 mm. For a combined load introduction according to ASTM D6641. Therefore, ± 45°C-GFRP tabs are applied with *UHU PLUS Endfest 300* (Uhu Holding GmbH, Bühl,Germany) at 60 °C. Ten specimen were tested per configuration.

2.5.3. Residual strength

A compression after impact (CAI) setup (ASTM D7137) is used to investigate the residual strength of flamed specimens on a *Allroundline Z400* (Zwick Roell, Ulm, Germany) with 1.25 mm/min. To exclude the influence of the particle modification on the mechanical properties, the residual strength was standardised to the compressive strength of unflamed specimens of the corresponding configuration (see Section 2.5.2). Sampling and loading positions are displayed in the supplementary information.

2.6. Microscopic examination

A digital microscope of type *VHX-6000* (Keyence Corporation, Osaka, Japan) is used for optical examination in several parts of this study. For quality control of manufacturing, parts of the plates for several configurations were embedded in *KEM 15 plus* (ATM Qness GmbH, Mammelzen, Germany) and polished with a polishing machine of type *Saphir 550* (ATM Qness GmbH, Mammelzen, Germany) prior to microscopy. Additional, microscopic fracture analysis after mechanical testing is conducted. Furthermore, specimens after flame-treatment were partially cut in the middle to examine their cross-sections. *ImageJ* was used to process and analyse these images.

Scanning electron microscopy (SEM) images were acquired with a SUPRA 55VP (Zeiss, Germany) using secondary electron (SE) detection with an accelerating voltage of 3 kV. Samples were cut with a CNC-saw and vaporised with gold for 30 s at 40 mA with a BALTEC SCD 050 SPUTTER (BALTIC Präparation e.K., Germany), creating an electrically conductive layer of a few nanometres thickness on the surface.

2.7. Quality control

Densities are measured with a precision scale *AT261 DeltaRange* equipped with a density determination kit (Mettler Toledo, Columbus, Ohio, USA), following Archimedes' principle for eight samples per configuration. Firstly, the mass of the specimen is weighed in air, followed by a measurement in ethanol. The difference between the two values corresponds to the buoyancy. Formula (1) is used to determine the density of the composite ρ_c, with A: weight in air, B: weight in ethanol and ρ_0: density of ethanol (at 21 °C: 0.78849 g/cm^3).

$$\rho_c = \frac{A}{A-B} \cdot \rho_0 \tag{1}$$

Fibre Volume ratios V_f are analysed based on ASTM D792-86 at 600 °C in a muffle furnance (Heraeus Deutschland GmbH & Co. KG, Hanau, Germany) for eight samples per configuration. V_f is calculated as displayed in (2), where v_f is the volume of the fibres and v_c the volume of the composite. According to data sheet information, the fibre density is $\rho_f = 2.62$ g/cm^3. The mass of the fibres (m_f) corresponds to the mass of the residuum after calcination and m_c/ρ_c is taken from density measurements.

$$V_f = \frac{v_f}{v_c} = \frac{\frac{m_f}{\rho_f}}{\frac{mc}{\rho_c}} \tag{2}$$

Table 1
Densities and fibre-volume ratios for all investigated configurations.

Configuration		Density in g/cm^3	Fibre-volume ratio in %
	Without NW	1.819 ± 0.004	45.2 ± 0.4
	With NW	1.825 ± 0.007	45.8 ± 0.4
*	*pre-cured	1.822 ± 0.008	45.5 ± 0.5
	1/8 6% RP	1.821 ± 0.010	45.3 ± 0.8
	1/8 12% RP	1.824 ± 0.007	45.7 ± 0.6
	1/4 12% RP	1.829 ± 0.006	46.1 ± 0.4

3. Results and discussion

3.1. Quality control of manufacturing

Filtration effects could be avoided by using the CPI method. As Fig. 3 exemplary shows, the RP particles remain in the desired plies, which can be detected by the red colour of the entire layers due to the red particles. Individual RP particles can be seen in Fig. 3 in white, as the particles scatter the light of the microscope. According to manufacturers' specifications, the median particle distribution is $D_{50} \approx 24$ µm. Larger particles in the range of approx. 50 µm are mainly present between the fibre layers and infiltrate the fibre bundles less frequently (see SEM image in the supplementary information). Due to the production of the prepregs via wet lay-up by hand, some pores are present in the prepreg layers. Porosity increased by a factor of ≈ 2.4, determined via analysis of digital microscopy images, as displayed in the supplementary information.

Densities and fibre-volume ratios are displayed in Table 1. The standard deviations within each configuration are very low, which indicates good reproducibility. The cured epoxy resin has a density of 1.16 g/cm^3, the glass-fibres 2.62 g/cm^3 and RP 2.2 g/cm^3. This explains the slightly higher density for the configuration with the highest particle loading and the lowest density without NW. Compared to the non-pre-cured, unmodified configuration, a slightly decreased density is observed in the pre-cured, non-modified configuration, due to the increased porosity occurring in hand-laminated pre-cured plies, but changes are within the standard deviations. Due to the closed RTM-mould with predetermined thickness of 4 mm, fibre-volume ratios are ≈ 45 % for all lay-ups. As expected, fibre-volume ratios are the lowest without NW. Hence, the manufacturing quality is adequate for the following investigations.

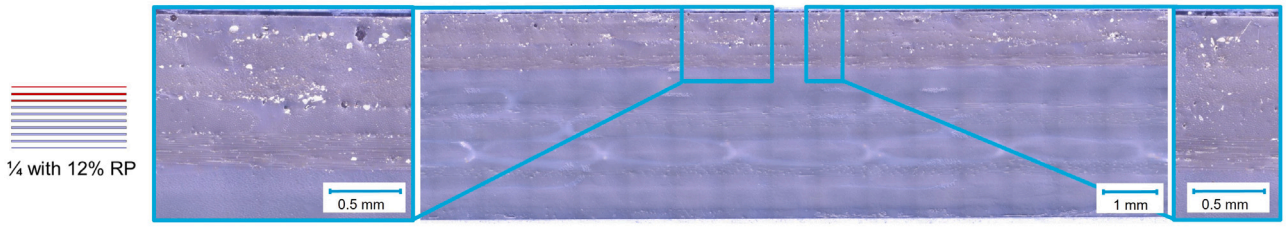

Fig. 3. Exemplary microscopic evaluation of CPI-process.

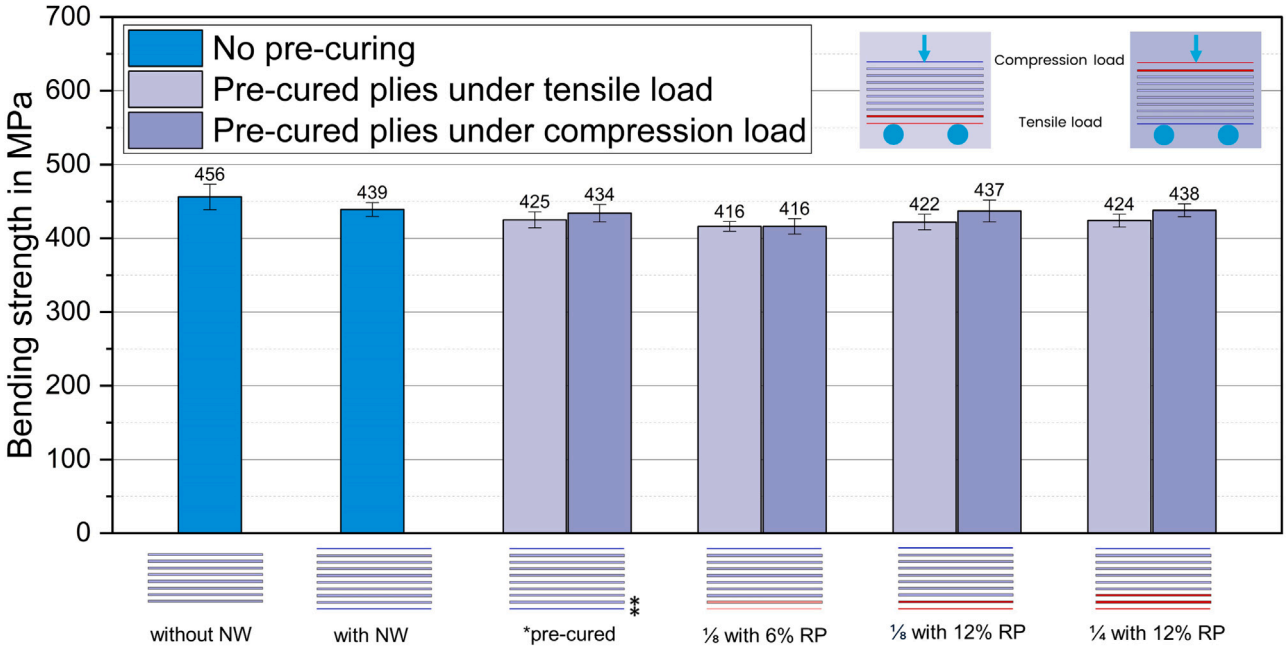

Fig. 4. Bending strengths for all configurations with the pre-cured side under tensile as well as under compressive load.

3.2. Impacts of CPI-process and particle loading on the bending strength

Fig. 4 displays the bending strengths for all investigated lay-ups. The plates manufactured with standard RTM-process are shown in blue. The NW reduces the bending strength due to a different fibre distribution over the cross-section resulting in a shifted *Steiner term*.

Within the lay-ups containing NWs, no difference exceeding the standard deviation could be found. In general, it is visible, that the bending strength measured with the pre-cured side under tensile load is slightly lower. Because this is the case for the unmodified but pre-cured configuration too, the decrease is supposed to be due to the occurring pores (see Section 3.1) rather than because of the implemented particles.

No further damage induced by the modified layers (e.g., delaminations during bending) were observed during the whole study.

3.3. Flame tests

The relative mass loss due to the flame treatment is shown in Fig. 5. The unmodified configuration without NW exhibits the greatest mass losses. The use of the NW already reduces mass losses. The matrix content is comparatively high in the NW, so more carbon is present, which can carbonise and form a char at the surface which acts as barrier against required components for flame maintenance like heat and oxygen.

The modification of the NW and 1/8 of the load-bearing plies with 6 wt. % RP only reduces the mass loss by a further small proportion. It is noticeable that the mass loss increases almost linearly with the flaming time, whereby the two configurations modified with 12 wt. % show less mass loss after 180 s, which may be an indicator of a desired delay. Another positive aspect is that the standard deviation is relatively low, ensuring that the flame test provides reproducible results.

Table 2 sums up the time-to-ignition and after-flame times after 180 s resp. 300 s flame treatment for different configurations. The trends are in line with the mass losses displayed in Fig. 5. The NW already delays the time to ignition (tti), while the after-flame times for both flame treatments were shortened. With 12 wt. % RP, significant improvements in tti were observed and further reductions in afterburning times, although the global RP content is still very low. By modifying the NW and 1/8 of the load-bearing layers with 6 wt. %, the analysed parameters, like the mass loss in Fig. 5, fall between the unmodified and the 12 wt. % modified values. One exception is the after-flame time after 300 s, which has already been reduced to a very low level. This may be due to the fact that a large part of the available matrix has already been carbonised over the entire cross-section and no further carbon source is available, causing the flame to fade. The unmodified test specimens also show lower afterburning times after 300 s than after 180 s, while the 12 wt. % modified lay-ups each show similar afterburning times in the range of 20 s. The supplementary information visualises the 180 s flame test, showing the significant improvement of the partial modified compared to the unmodified configuration.

The discussed trends are predominantly beyond the standard deviations of the investigated parameters (see Table 2). While the standard deviations of the unmodified configurations show higher deviations, e.g., in their after-flame times after 180 s flame treatment, the configuration with the highest degree of modification (¼ 12% RP) shows very

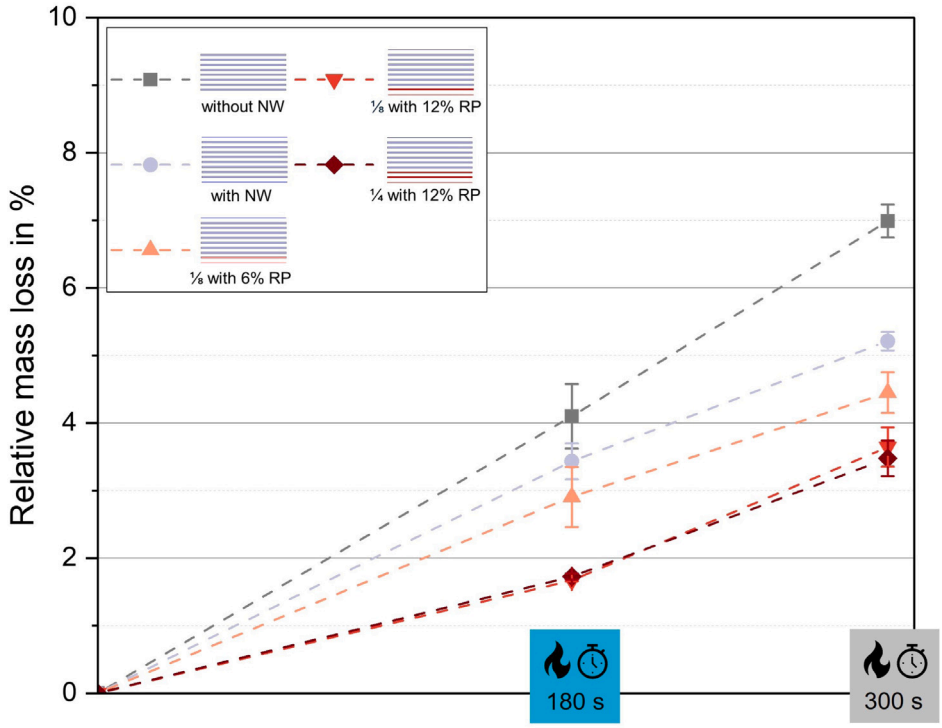

Fig. 5. Relative mass loss in % for different lay-ups and 180 s as well as 300 s of flame treatment.

Table 2
Time-to-ignition and after-flame times after 180 s resp. 300 s flame treatment for n = 4 specimens of different configurations.

Configuration	Time-to-ignition in s	after-flame time in s (180 s flame)	after-flame time in s (300 s flame)
Without NW	14.6 ± 1.2	55.0 ± 17.1	27.5 ± 4.0
With NW	16.0 ± 2.8	50.0 ± 16.1	30.3 ± 2.9
⅛ 6% RP	20.4 ± 2.4	32.5 ± 2.5	18.0 ± 5.4
⅛ 12% RP	24.6 ± 10.1	23.0 ± 6.8	22.3 ± 4.9
¼ 12% RP	37.3 ± 2.5	20.3 ± 2.9	18.7 ± 0.5

repeatable results in their time-to-ignition and after-flame times. Despite the simplicity of the tests and the complexity of fire development processes, the tailored flame tests can be classified as representative and reproducible.

In Fig. 6 cross sections after flame treatment are shown which confirm, that the whole cross-section is affected for the unmodified and 6 wt. % configurations. The higher mass loss for unmodified specimens (Fig. 5) is due to a broader affected area without RP.

Fig. 6 (right) shows the affected areas of test specimens from the flamed and unflamed side. The modification with FR leads to a typical reaction of the RP with O_2 and H_2O from the air on the flamed side to condensed phosphoric acid at approx. 300 °C, which forms a protective layer (see Fig. 6, bottom right). The unflamed side is already damaged for unmodified specimens after 180 s of flame exposure, while the modified configuration under consideration shows a brown discolouration in a limited area due to the heat exposure. The fibres are still intact, which can also be seen in the cross-sections in Fig. 6 (left).

In Fig. 7, the temperature progression over time is displayed for the flamed surface aside from the flame. It can be seen, that the measured temperature decreases with increasing amount of RP. As described, the char which is build with RP slows down the heat transfer, resulting in lower temperatures at the edge of the specimen. Consequently, the area with critical high temperatures for matrix degradation decrease with the use of RP.

3.4. Residual compressive strength after flame tests

Fig. 8 shows the residual strength of the different lay-ups standardised to their compressive strength (see Table A.1, Appendix). To exclude influences from manufacturing, the unmodified specimen are also manufactured via CPI-method.

The residual strength of the specimens modified with 6 wt. % RP is on the same low level as for unmodified specimen. This observation

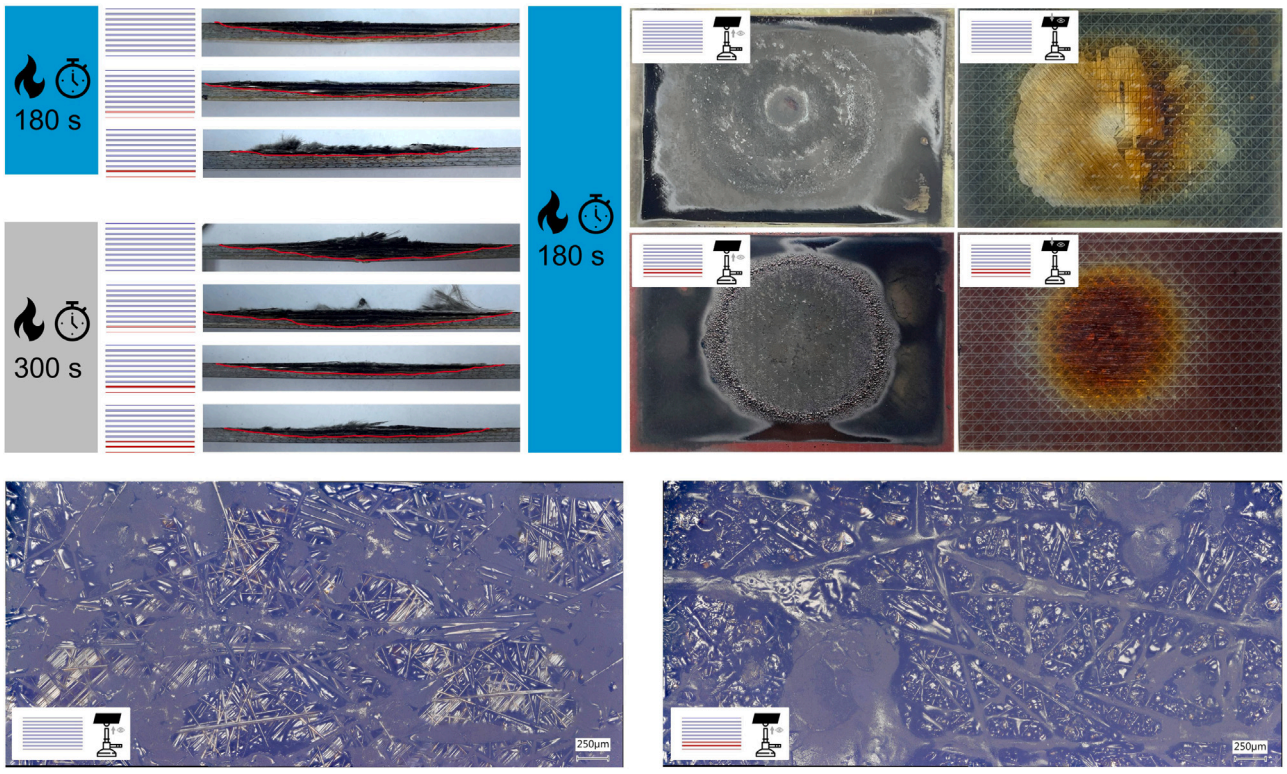

Fig. 6. Top left: Cross-sections of relevant configurations after flame tests. Influenced plies are marked. Top right: Flamed and opposite surfaces of specimens after 180 s flame treatment. Bottom left: Blank NW without RP modification. Bottom right: NW with char of condensed phosphoric acid.

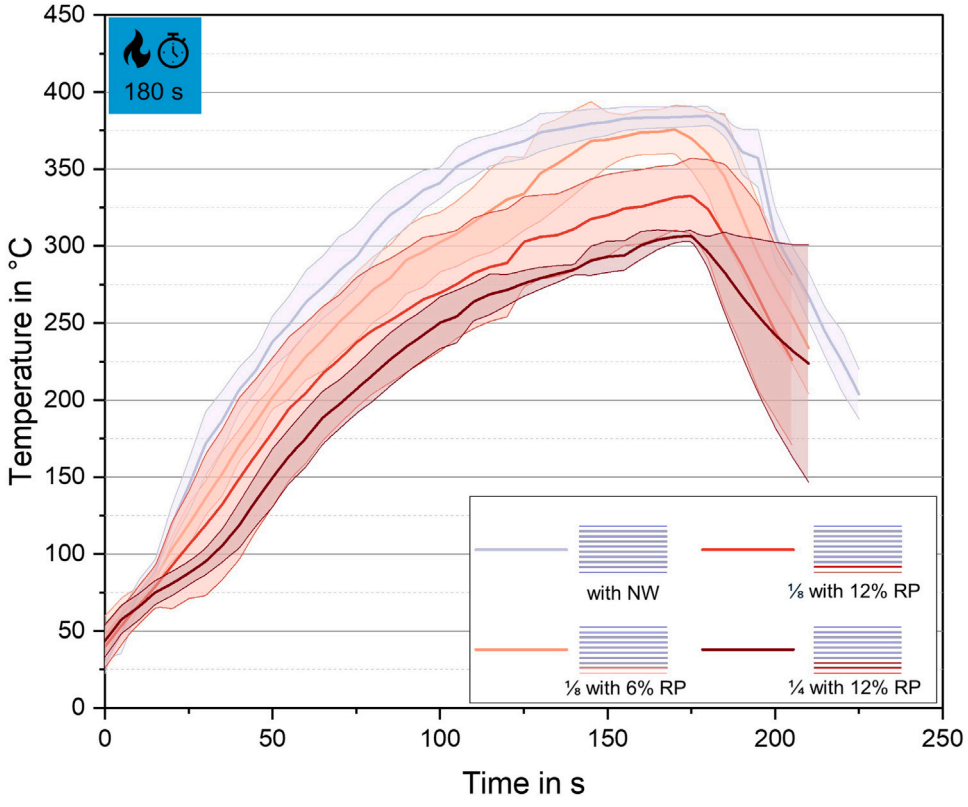

Fig. 7. Temperature of sensor on the flamed side during 180 s flame test for different lay-ups.

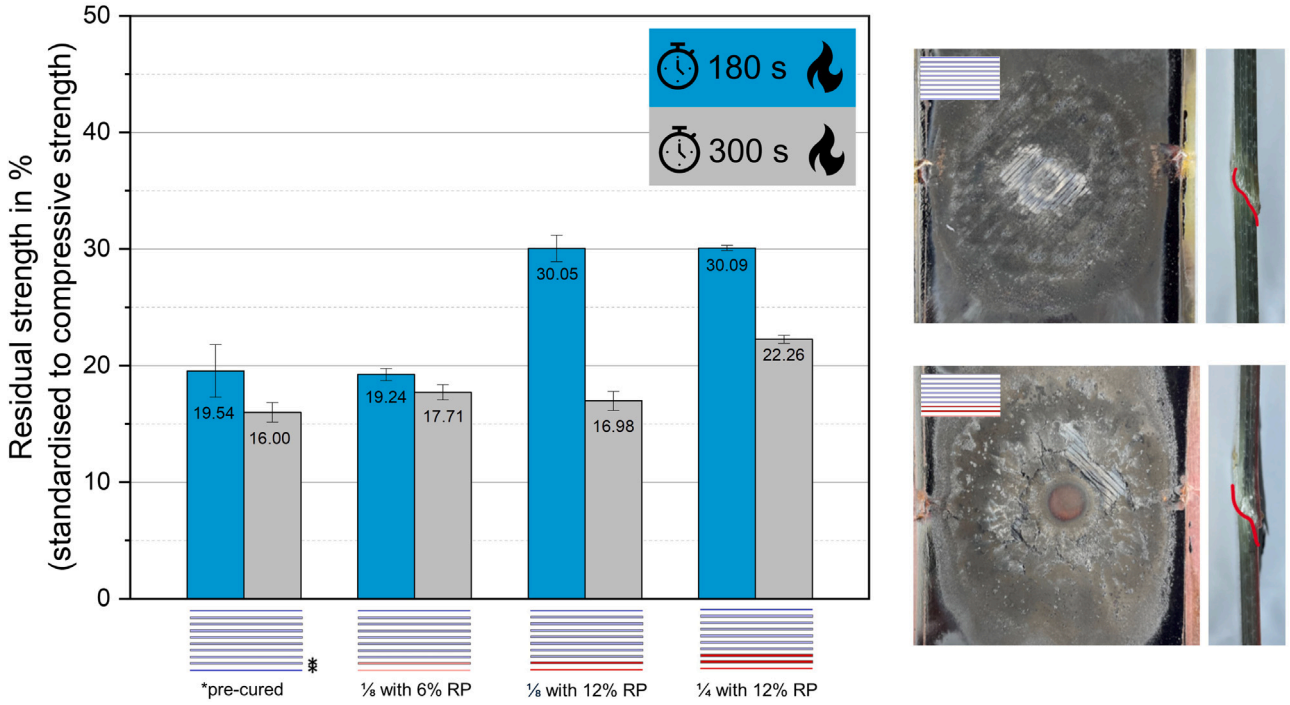

Fig. 8. Compressive strength retention of n = 3 specimens after flame tests and specimens after testing.

is in line with the affected plies shown in Fig. 6, where for both lay-ups similar levels of damage are visible. The modification of 1/8 of the load bearing plies with 12 wt.% RP significantly improves the residual strength after 180 s of flame treatment while after 300 s of fire load, the compressive strength drops to the low values of the first discussed configurations.

The residual compressive strength of the composites containing 12 wt. % RP is up to 54 % higher after 180 s flame tests compared to the non- and low-modified composites, while the highest modification grade (1/4 12 %) also increased the residual strength after 300 s flame treatment by about 40 %. These results highlight the significant improvement due to the local modification.

The differences in the residual compressive strengths of the different configurations fall outside the standard deviations and are therefore reproducible for several specimens (n = 3). As the compressive strength retention is highly influenced by the sample destruction by the flame treatment (see cross-sections in Fig. 6), the standard deviation for the compressive strength retention is slightly higher for specimens, where the standard deviations in Table 2, e.g., after-flame times, were higher too.

As the pictures in Fig. 6 show, the char which is build during flame test with RP-modification cracks under compressive load and unembedded fibres become visible underneath, wherein load transfer is limited resulting in lower compressive strengths. A micrograph of a char crack is displayed in the supplementary information, showing, that the cracks occur in the condensed phosphoric acid char in the NW (also see Fig. 6). Accordingly, this char layer initially bears minimal loads compared to the blank NW without RP modification, where no cracks occur. However, compared to the fibres with intact matrix, this is only expected to be a very small proportion.

The proportion of plies with degraded matrix is accordingly decisive for the residual strength. Of course, the ≈ 30 % residual compressive strength determined in this study is generally not sufficient for further operation. However, in contrast to e.g. impact damages [47], fires are easily noticable and components are replaced after the fire. Nevertheless, an improved residual strength increases the probability of being able to evacuate in the event of a fire.

The test setup for determining the residual strength is therefore suitable for making qualitative comparisons between the examined configurations for uniform flame treatments. It reveals significant improvements with only small global amounts of RP when concentrated at the fire loaded surface. However, the number of modified plies has to be adjusted for specific applications to fulfil all requirements to pass demanded large-scale tests.

4. Conclusions

The combination of RTM and prepregs with FR particles enables an industrially feasible production method with low total FR content (≈ 1.5 - 3 % RP) and improves flame retardancy and residual strength. In addition, reduced FR contents not only save material, but also minimise negative effects such as reduced mechanical properties.

The presented approach provides clear results for evaluating flame retardancy and residual strength using minimal equipment. The developed screening method allows qualitative comparisons to be made between different laminates and acts as a supplement to the more complex, standardised test methods.

In industrial use, flame-retardant modified prepregs can be positioned in RTM moulds in an automated manner, allowing the manufacturing of large parts, e.g., train walls, in infusion processes, but implementing the flame retardancy directly in the load-bearing plies. Therefore, this method can contribute to reducing weight in mobility applications by saving the weight of flame retardant gel-coats or coatings, respectively allowing additional functionalities using gel-coats. For certification in industrial applications, the number of modified plies has to be adjusted to pass the respective standards.

CRediT authorship contribution statement

Melissa Walter: Writing – original draft, Visualization, Project administration, Methodology, Investigation, Formal analysis, Conceptualization. **Antonia Jarchow:** Writing – review & editing, Investigation. **Bodo Fiedler:** Writing – review & editing, Supervision, Project administration, Funding acquisition, Conceptualization.

Declaration of competing interest

The authors declare that they have no known competing financial interests or personal relationships that could have appeared to influence the work reported in this paper.

Acknowledgements

Publishing fees supported by Funding Programme Open Access Publishing of Hamburg University of Technology (TUHH). The authors would like to thank the Ingeborg Gross Foundation for financial support and all colleagues for helpful discussions, especially Fabian Riebesehl for his support during the acquisition of SEM images.

Appendix A

See Table A.1

Table A.1
Compressive strengths of relevant configurations.

Configuration		Compressive strength in MPa
	*pre-cured	390.09 ± 11.95
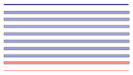	1/8 6% RP	379.84 ± 13.22
	1/8 12% RP	400.94 ± 22.93
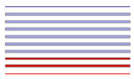	1/4 12% RP	422.96 ± 15.52

Appendix B. Supplementary data

Supplementary material related to this article can be found online at https://doi.org/10.1016/j.compositesa.2025.109339.

Data availability

Data will be made available on request.

References

[1] Hsiao K-T, Heider D. 10 - vacuum assisted resin transfer molding (VARTM) in polymer matrix composites. In: Advani SG, Hsiao K-T, editors. Manufacturing techniques for polymer matrix composites (pMCs). Woodhead publishing series in composites science and engineering, Woodhead Publishing; 2012, p. 310–47. http://dx.doi.org/10.1533/9780857096258.3.310.

[2] Bodaghi M, Costa R, Gomes R, Silva J, Correia N, Silva F. Experimental comparative study of the variants of high-temperature vacuum-assisted resin transfer moulding. Compos Part A: Appl Sci Manuf 2020;129:105708. http://dx.doi.org/10.1016/j.compositesa.2019.105708.

[3] Xiao W, He P, Hu G, He B. Study on the flame-retardance and thermal stability of the acid anhydride-cured epoxy resin flame-retarded by triphenyl phosphate and hydrated alumina. J Fire Sci 2001;19(5):369–77. http://dx.doi.org/10.1106/R4HN-GT2G-EWAR-733C.

[4] Levchik SV, Weil ED. Thermal decomposition, combustion and flame–retardancy of epoxy resins—a review of the recent literature. Polym Int 2004;53(12):1901–29. http://dx.doi.org/10.1002/pi.1473.

[5] Hayes BS, Seferis JC. Modification of thermosetting resins and composites through preformed polymer particles: A review. Polym Compos 2001;22(4):451–67. http://dx.doi.org/10.1002/pc.10551.

[6] Kinloch AJ, Masania K, Taylor AC, Sprenger S, Egan D. The fracture of glass-fibre-reinforced epoxy composites using nanoparticle-modified matrices. J Mater Sci 2008;43(3):1151–4. http://dx.doi.org/10.1007/s10853-007-2390-3.

[7] Lefevre D, Comas-Cardona S, Binétruy C, Krawczak P. Modelling the flow of particle-filled resin through a fibrous preform in liquid composite molding technologies. Compos Part A: Appl Sci Manuf 2007;38(10):2154–63. http://dx.doi.org/10.1016/j.compositesa.2007.06.008.

[8] Giannakopoulos G, Masania K, Taylor AC. Toughening of epoxy using core–shell particles. J Mater Sci 2011;46(2):327–38. http://dx.doi.org/10.1007/s10853-010-4816-6.

[9] Da Reia Costa EF, Skordos AA, Partridge IK, Rezai A. RTM processing and electrical performance of carbon nanotube modified epoxy/fibre composites. Compos Part A: Appl Sci Manuf 2012;43(4):593–602. http://dx.doi.org/10.1016/j.compositesa.2011.12.019.

[10] Louis BM, Maldonado J, Klunker F, Ermanni P. Particle distribution from in–plane resin flow in a resin transfer molding process. Polym Eng Sci 2019;59(1):22–34. http://dx.doi.org/10.1002/pen.24860.

[11] Lefevre D, Comas-Cardona S, Binetruy C, Krawczak P. Coupling filtration and flow during liquid composite molding: Experimental investigation and simulation. Compos Sci Technol 2009;69(13):2127–34. http://dx.doi.org/10.1016/j.compscitech.2009.05.008.

[12] Fan Z, Advani SG. Capillary effect of multi-walled carbon nanotubes suspension in composite processing. J Nanosci Nanotechnol 2008;8(4):1669–78.

[13] Shekarchi M, Farahani EM, Yekrangnia M, Ozbakkaloglu T. Mechanical strength of CFRP and GFRP composites filled with APP fire retardant powder exposed to elevated temperature. Fire Saf J 2020;115:103178. http://dx.doi.org/10.1016/j.firesaf.2020.103178.

[14] Bar M, Alagirusamy R, Das A. Flame retardant polymer composites. Fibers Polym 2015;16(4):705–17. http://dx.doi.org/10.1007/s12221-015-0705-6.

[15] Petersen MR, Chen, Roll M, Jung SJ, Yossef M. Mechanical properties of fire-retardant glass fiber-reinforced polymer materials with alumina tri-hydrate filler. Compos Part B: Eng 2015;78:109–21. http://dx.doi.org/10.1016/j.compositesb.2015.03.071.

[16] Liang JZ, Feng JQ, Tsui CP, Tang CY, Liu DF, Zhang SD, Huang WF. Mechanical properties and flame-retardant of PP/MRP/$Mg(OH)_2$/$Al(OH)_3$ composites. Compos Part B: Eng 2015;71:74–81. http://dx.doi.org/10.1016/j.compositesb.2014.10.054.

[17] Ameen F, Atif M, Mahmood K, Yousuf UF. Qualitative and quantitative impact of filler on thermomechanical properties of epoxy composites. Polym Adv Technol 2021;32(8):2813–28. http://dx.doi.org/10.1002/pat.5304.

[18] Choudhary M, Singh T, Dwivedi M, Patnaik A. Waste marble dust–filled glass fiber–reinforced polymer composite part I: Physical, thermomechanical, and erosive wear properties. Polym Compos 2019;40(10):4113–24. http://dx.doi.org/10.1002/pc.25272.

[19] Sharma H, Kumar A, Rana S, Sahoo NG, Jamil M, Kumar R, Sharma S, Li C, Kumar A, Eldin SM, Abbas M. Critical review on advancements on the fiber-reinforced composites: Role of fiber/matrix modification on the performance of the fibrous composites. J Mater Res Technol 2023;26:2975–3002. http://dx.doi.org/10.1016/j.jmrt.2023.08.036.

[20] Trubachev S, Paletsky A, Sosnin E, Tuzhikov O, Buravov B, Shmakov A, Chernov A, Kulikov I, Sagitov A, Hu Y, Wang X. Flame-retardant glass fiber-reinforced epoxy resins with phosphorus-containing bio-based benzoxazines and graphene. Polymers 2024;16(16). http://dx.doi.org/10.3390/polym16162333.

[21] Yang J-X, Sun Y, Song W-M, Liu Y. A novel phosphorus/boron-containing flame retardant for improving the flame retardancy of ramie fiber reinforced epoxy composites. Constr Build Mater 2024;451:138814. http://dx.doi.org/10.1016/j.conbuildmat.2024.138814.

[22] Mi Z, Chu F, Hu W, Hu Y, Song L. Eco-friendly preparation of advanced epoxy composites and their pyrolysis and flame retardant mechanisms. Polym Degrad Stab 2024;224:110749. http://dx.doi.org/10.1016/j.polymdegradstab.2024.110749.

[23] Murad MS, Hamzat AK, Asmatulu E, Asmatulu R. Flame-retardant fiber composites: synergistic effects of additives on mechanical, thermal, chemical, and structural properties. Adv Compos Hybrid Mater 2025;8(1). http://dx.doi.org/10.1007/s42114-024-01111-1.

[24] Zhao Z, Qu J, Geng Y, Li R, Qiu J, Liu M, Chen X, Li S, Jiao C. Facile preparation of microcapsuled P-N@MXene flame retardant using layer-by-layer assembly strategy towards enhanced fire safety of epoxy resin. Polym Degrad Stab 2025;234:111219. http://dx.doi.org/10.1016/j.polymdegradstab.2025.111219.

[25] Liu C, Tao J, Wu T, Zhao H-B, Yu C, Rao W. Construction of hierarchical SiO2 microcapsule towards flame retardation, low toxicity and mechanical enhancement of epoxy resins. Chemosphere 2023;342:140184. http://dx.doi.org/10.1016/j.chemosphere.2023.140184.

[26] Zhao M, Guo N, Wang K, Qu Q, Zhang Q, Wang C, Xin H. Facial functionalization carbon fiber with MnO 2 nanosheets for high–performance epoxy composites with excellent flame retardancy and mechanical properties. Polym Compos 2025;46(8):7569–80. http://dx.doi.org/10.1002/pc.29450.

[27] Muralidharan ND, Subramanian J, Rajamanickam SK, Krishnasamy P, Thiagamani SMK, Khan A. Flame retardant characteristics of natural fibre reinforced polymer composites: A thematic review. Polym Compos 2024;45(14):12530–58. http://dx.doi.org/10.1002/pc.28699.

[28] Yu M, Chu Y, Xie W, Fang L, Liu X, Zhang O, Ren M, Sun J. An interlayer flame retardant method to effectively fire retardant and reinforce CF/EP composites by nanofiber film intercalation. Chem Eng J 2023;467:143545. http://dx.doi.org/10.1016/j.cej.2023.143545.
[29] Shi X-H, Li X-L, Li Y-M, Li Z, Wang D-Y. Flame-retardant strategy and mechanism of fiber reinforced polymeric composite: A review. Compos Part B: Eng 2022;233:109663. http://dx.doi.org/10.1016/j.compositesb.2022.109663.
[30] Pomázi Á, Toldy A. Multifunctional gelcoats for fiber reinforced composites. Coatings 2019;9(3):173. http://dx.doi.org/10.3390/coatings9030173.
[31] Pomázi Á, Krecz M, Toldy A. Thermal behaviour and fire and mechanical performance of carbon fibre-reinforced epoxy composites coated with flame-retardant epoxy gelcoats. J Therm Anal Calorim 2023;148(7):2685–702. http://dx.doi.org/10.1007/s10973-022-11710-z.
[32] Zhang L, Ren H, Wu L, Liu Z, Xie A, Yao X, Ju J, Liu M. Recent advances in gel coatings: from lab to industry. J Mater Chem A 2024;12(30):18901–20. http://dx.doi.org/10.1039/D4TA02586E.
[33] Xu W, Gu Y, Li M, Ma X, Zhang D, Zhang Z. Co-curing process combining resin film infusion with prepreg and co-cured interlaminar properties of carbon fiber composites. J Compos Mater 2014;48(14):1709–24. http://dx.doi.org/10.1177/0021998313490536.
[34] Di Fratta C, Mario D, Gabathuler V, Zogg M, Ermanni P. Approach to optimizing a combined out-of-autoclave (OOA) prepreg/liquid composite molding (LCM) process for integrated structures. Sampe J 2012;48:40–6.
[35] Kaps R, Wiedemann M. Combined prepreg and resin infusion technologies. In: Wiedemann M, editor. Adaptive, tolerant and efficient composite structures. Research topics in aerospace, Berlin and Heidelberg: Springer; 2013, p. 349–61. http://dx.doi.org/10.1007/978-3-642-29190-6_28.
[36] Katunin A, Danek W, Wronkowicz A, Dragan K. Methodology of residual strength prediction of composite structures with low-velocity impact damage based on NDT inspections and numerical-experimental CAI testing. Int J Impact Eng 2023;181:104762. http://dx.doi.org/10.1016/j.ijimpeng.2023.104762.
[37] Körbelin J, Dreiner C, Fiedler B. Impact of temperature on LVI-damage and tensile and compressive residual strength of CFRP. Compos Part C: Open Access 2020;3:100074. http://dx.doi.org/10.1016/j.jcomc.2020.100074.
[38] Agrawal A, Kodur V. Residual response of fire–damaged high–strength concrete beams. Fire Mater 2019;43(3):310–22. http://dx.doi.org/10.1002/fam.2702.
[39] Li H-T, Young B. Residual mechanical properties of high strength steels after exposure to fire. J Constr Steel Res 2018;148:562–71. http://dx.doi.org/10.1016/j.jcsr.2018.05.028.
[40] Yang J, Ji C, Wang D, Zhang H, Zhou Z, Hu J, Wang B. Fire behavior and post-fire residual tensile strength prediction of carbon fiber/phthalonitrile composite laminates. Compos Sci Technol 2024;252:110624. http://dx.doi.org/10.1016/j.compscitech.2024.110624.
[41] Vieille B, Coppalle A, Le Pluart L, Schuhler E, Chaudhary A, Rijal B, Alia A, Delpouve N, Bourdet A. Influence of a flame-retardant on the fire-behaviour and the residual mechanical properties of C/PEKK composite laminates exposed to a kerosene flame. Compos Part A: Appl Sci Manuf 2022;152:106720. http://dx.doi.org/10.1016/j.compositesa.2021.106720.
[42] Sorathia U, Beck C, Dapp T. Residual strength of composites during and after fire exposure. J Fire Sci 1993;11(3):255–70. http://dx.doi.org/10.1177/073490419301100305.
[43] Millen S, Xu X, Lee J, Mukhopadhyay S, Wisnom MR, Murphy A. Towards a virtual test framework to predict residual compressive strength after lightning strikes. Compos Part A: Appl Sci Manuf 2023;174:107712. http://dx.doi.org/10.1016/j.compositesa.2023.107712.
[44] Wang FS, Yu XS, Jia SQ, Li P. Experimental and numerical study on residual strength of aircraft carbon/epoxy composite after lightning strike. Aerosp Sci Technol 2018;75:304–14. http://dx.doi.org/10.1016/j.ast.2018.01.029.
[45] Walter M, Jarchow A, Fiedler B. Heterogeneously distributed flame retardants in fibre-reinforced epoxies: Novel manufacturing process and tailored flame tests. In: Christophe Binetruy, Jacquemin F, editors. Proceedings of the 21st European conference on composite materials: nantes université. 3, 2024, p. 93–100.
[46] Walter M, Neubacher M, Fiedler B. Using thermokinetic methods to enhance properties of epoxy resins with amino acids as biobased curing agents by achieving full crosslinking. Sci Rep 2024;14(1):4367. http://dx.doi.org/10.1038/s41598-024-54484-0.
[47] Körbelin J. Damage tolerance of high-performance composites (Ph.D. thesis), Hamburg: Institute of Polymers; 2022, http://dx.doi.org/10.15480/882.4276.